



Article

Mechanical Properties and Damage Characteristics of Coal-Based Solid Waste Paste Filling Materials with Different Moisture Content

Meng Wang ^{1,2}, **Xiang He** ^{2,3,*} and **Ke Yang** ^{1,2,3}¹ School of Mining Engineering, Anhui University of Science and Technology, Huainan 232001, China² Institute of Energy, Hefei Comprehensive National Science Center, Hefei 230031, China³ State Key Laboratory of Mining Response and Disaster Prevention and Control in Deep Coal Mine, Anhui University of Science and Technology, Huainan 232001, China

* Correspondence: xianghe_cumtb@126.com

Abstract: It has been proven that it is a feasible treatment method to prepare paste filling material from coal-based solid waste to fill underground goaf. Based on the complexity of the goaf environment, especially the influence of humidity on paste filling materials, this paper prepared paste filling materials with a mass concentration of 80% by using coal gangue and fly ash, and carried out a uniaxial compression test of coal-based solid waste paste filling materials under four different water-bearing states. The experimental results show that: (1) The binary primary equation fits well the variation trend of paste filling strength with water content. With the increase of moisture content, the compressive strength of paste filling material gradually decreases, and the higher the moisture content, the more obvious the influence on the strength of paste filling. (2) The damage evolution equation and constitutive equation of paste filling materials with different moisture content were established. With the increase of strain, the influence of moisture content on the damage of paste filling material decreases gradually, and the moisture content can promote the damage development of paste filling material to a certain extent. (3) The influence mechanism of moisture content on coal based-solid waste paste filling material is discussed from the three aspects of physical effect, structural effect and chemical effect, which provides a direction for further research on the influence mechanism of moisture content on filling strength. The research on the failure mechanism of coal-based solid waste paste filling and the safety production of the mine can be used as a theoretical support.



Citation: Wang, M.; He, X.; Yang, K. Mechanical Properties and Damage Characteristics of Coal-Based Solid Waste Paste Filling Materials with Different Moisture Content. *Sustainability* **2023**, *15*, 1523. <https://doi.org/10.3390/su15021523>

Academic Editor: Guang-Liang Feng

Received: 29 November 2022

Revised: 4 January 2023

Accepted: 9 January 2023

Published: 12 January 2023



Copyright: © 2023 by the authors. Licensee MDPI, Basel, Switzerland. This article is an open access article distributed under the terms and conditions of the Creative Commons Attribution (CC BY) license (<https://creativecommons.org/licenses/by/4.0/>).

1. Introduction

The accumulation of solid wastes such as coal gangue and fly ash generated by coal mining on the ground not only occupies a large amount of land surface but also seriously pollutes the ecological environment [1,2]. It is a feasible method to backfill underground under the premise of ensuring no pollution of solid waste [3]. Since the 21st century, with the increasing problem of “three under” coal pressure and the continuous proposal of national environmental protection policies, solid filling [4,5], paste filling [6,7], separation grouting [8,9] and other technologies have become the trend of green mining in coal mines. Using coal-based solid wastes to prepare paste filling materials for paste filling mining has become an important development direction of “green mine” construction [10–12]. However, due to the depletion of shallow coal resources, coal mining began to move deeper. The complex geological conditions of deep coal mining and the great changes in goaf humidity and temperature have become the restricting factors for paste filling mining [13]. There have been many studies on multi-field coupling such as rock mass [14,15], and paste filling materials are also subject to multi-field interaction in goaf. Therefore, the effect of

humidity on the strength and damage of the paste filling in goaf was of great significance to study.

Under laboratory conditions, the transportation and emergency stop of backfill mixture prepared based on water soluble ore-concentrated waste under different water solid ratios were simulated [16]. References [17–19] carried out uniaxial compression tests of cemented tailings filling under different curing ages, loading rates and mixed aggregates, analyzed pre-peak and post-peak damage and energy consumption characteristics of cemented tailings filling under different curing ages, loading rates and mixed aggregates, and expounded its evolution process. References [20–22] carried out uniaxial compression tests for gangue cemented filling with different sizes, early load and width-to-height ratio, analyzed the impact of size effect, early load and width-to-height ratio on filling strength, acoustic emission characteristics, resistivity and damage, and characterized the damage evolution process of filling based on the changes of acoustic emission ringing number and resistivity. Reference [23] used five kinds of coal-based solid wastes, such as coal gangue, fly ash, desulfurized gypsum, furnace bottom slag and gasification slag to prepare filling materials, carried out research on the strength and acoustic emission characteristics of filling specimens in different phases, and revealed the evolution law of filling strength based on the microstructure of specimens. Reference [24], based on acoustic emission, studied the damage mechanical characteristics and cooperative deformation mechanism of tailings cemented filling and different lime sand ratio combinations under uniaxial compression. Based on the statistical damage theory, strain equivalent hypothesis and maximum tensile stress criterion, reference [25] introduced the damage constitutive model of cemented tailing filling under uniaxial compression, and established the damage constitutive model modified by compaction process. Reference [26] studied the influence of curing temperature on shear failure of the cementing surface between filling and surrounding rock, and analyzed the internal mechanism of the influence of curing temperature on mechanical properties of the cementing surface between filling and surrounding rock. Based on DIC technology, reference [27] obtained the main strain nebulae of filling specimen when it was damaged, and analyzed the snatch characteristics and damage failure characteristics of tailings filling with different particle size distributions. Reference [28] analyzed the strength evolution mechanism of tailings filling under different curing pressures by binarization treatment of electron microscope scanning images and application of fractal theory. In terms of the influence of humidity on filling in complex geological environment, reference [29] carried out uniaxial compressive tests of full tailings cemented filling with different water content, and analyzed the relationship between its strength and damage with water content. Reference [30] studied the mechanical properties of cemented filling under different water saturations, and built the damage constitutive model of cemented filling under different water saturations based on Lemaitre strain equivalence principle and Weibull distribution. Reference [31] carried out uniaxial compression tests for two kinds of tailings paste filling materials with different cement contents, and analyzed the influence law of water content on the strength, elastic modulus and peak strain point of the filling materials. Reference [32] carried out triaxial creep tests of gangue cemented filling materials under different moisture content, analyzed the influence of moisture content on the creep rate, long-term deformation and strength of the filling body, and established a fractional creep model to describe the whole creep process.

To sum up, although many researchers have studied the strength and damage of paste filling, the research on the damage mechanism of coal-based solid waste paste filling caused by moisture content is still not perfect. Based on this, the paper takes coal gangue as aggregate, fly ash and cement as cementitious materials, prepares paste filling specimens with a concentration of 80%, carries out research on the strength characteristics of paste filling under different water content, establishes a damage constitutive model based on water content, and the influence mechanism of water content on filling body strength and failure form is further discussed from the physical, structural and chemical perspectives.

This study provides a theoretical reference for further discussing the damage mechanism of water content to coal-based solid waste paste filling and the safety production of the mine.

2. Experimental Methods

2.1. Physical and Chemical Property Analysis

The cement was ordinary Portland cement, the fly ash was Grade II fly ash from Yuanyanghu Power Plant in Ningdong Coal Power Base, and the coal gangue was from Renjiazhuang Coal Mine of Ningxia Coal Industry Co., Ltd. of National Energy Group, Ningxia Autonomous Region, China. SEM and XRD analysis can be used to analyze the existence of new formations and the presence of strong bonds in the new composite materials formed [33]. FlexSEM 1000 (Hitachi, Tokyo, Japan) and SmartLab SE (Rigaku, Tokyo, Japan) instruments were used for SEM and XRD analysis, respectively. The scanning speed of XRD is 4° /min, the range is $5\text{--}70^\circ$, and the continuous scanning mode is adopted. Physical and chemical properties of coal gangue and fly ash are shown in Figure 1.

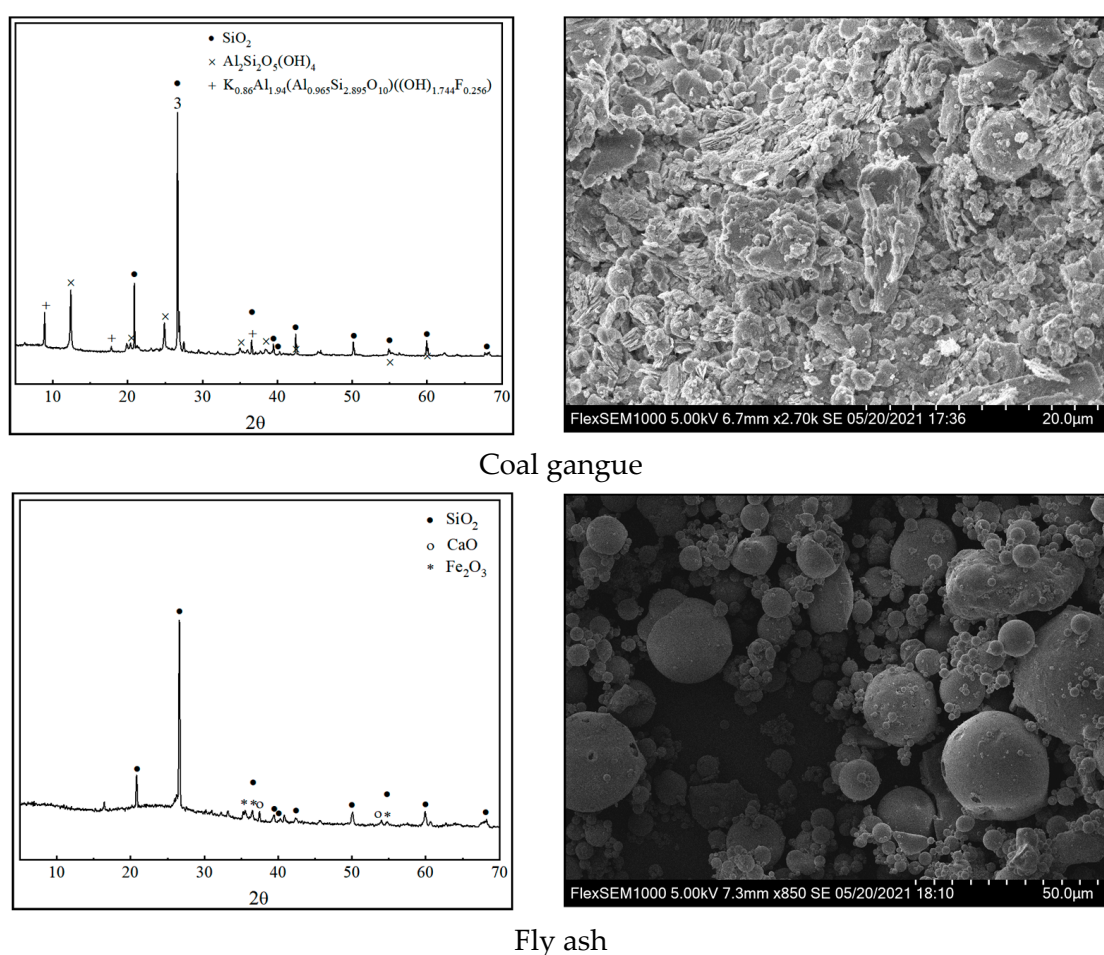


Figure 1. SEM and XRD analysis of coal gangue and fly ash.

Coal gangue comes from solid waste discharged during coal mining or coal washing. It is a black gray rock with lower carbon content and harder than coal in the process of coal forming. According to SEM and XRD in Figure 1, the micro morphology of coal gangue is irregular, such as block or sheet, which is not easy to flow on the static plane. The largest diffraction peak appears in the diffraction pattern of coal gangue samples between $20^\circ\text{--}30^\circ$, indicating that the crystalline mineral composition in coal gangue is mainly SiO_2 , and the content of other crystalline minerals such as CaO and Fe_2O_3 is less.

Fly ash is formed by the absorption and cooling of the heating surface of pulverized coal during suspension combustion in a furnace at $1300\text{--}1500^\circ\text{C}$ and its particle size is

generally between 1~100 μm . According to SEM and XRD in Figure 1, the microstructure of fly ash is relatively regular, showing spherical particles of different sizes, which increases the migration and flow of fly ash and is convenient to pass through the pores between large particles. The largest diffraction peak appears in the diffraction pattern of fly ash samples between $20^\circ\sim30^\circ$, indicating that the crystalline mineral composition in fly ash is mainly SiO_2 , and the content of other crystalline minerals is less.

2.2. Preparation of Filling Specimen

By changing the ratio and mass concentration, the activation characteristics of the composite can be conditioned, and then the strength characteristics of the backfill can be affected [34]. Coal-based solid waste was used to prepare paste filling materials, and coal gangue was selected as aggregate, fly ash and cement as cementing materials. Ordinary Portland cement is used as the cement, which has fast hydration reaction and high early and late strength. Paste filling specimens with a mass concentration of 80% were prepared according to the ratio of coal gangue: fly ash:cement:water = 5:2:1:2 [35,36]. The coal gangue was crushed and screened (particle size was 0~15 mm). During preparation, add coal gangue, fly ash and cement in the mixing tank according to the set proportion, and stir them fully, so that the coal gangue, fly ash and cement are fully mixed. After complete mixing, add a set proportion of water into the mixing tank and stir thoroughly for 15 min. Then poured into a cylindrical abrasive with a diameter of 50 mm and a height of 100 mm, demoulded 24 h later, and then immediately placed in an HBY-60B standard constant temperature and humidity curing box for 28 d, curing humidity was 95%, curing temperature was $20 \pm 1^\circ\text{C}$. A total of 12 paste specimens were prepared. Each moisture content was tested three times, and the average value of the three results was used as the experimental value to ensure the accuracy of the experimental results. The sample preparation process was shown in Figure 2.

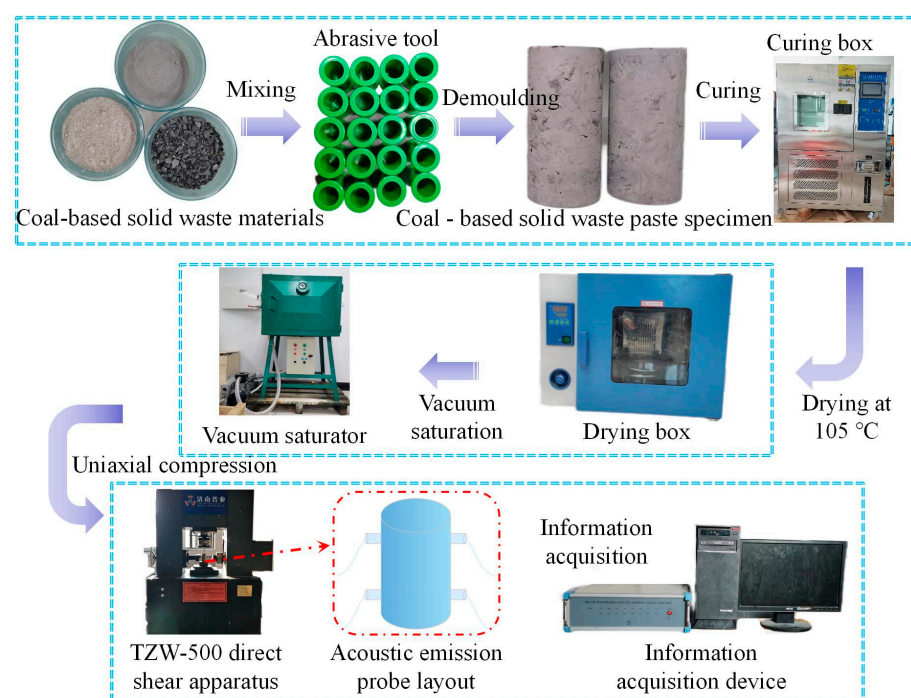


Figure 2. Experimental setup and procedure.

The curing filling specimen was put into the drying box, dried at 105°C for 24 h, and weighed and recorded. Then, the dried filling specimens were divided into four groups: A, B, C, and D. Group A was the dried specimen, and group B, C, and D were saturated with water for 1 h, 2 h, and 4 h, respectively (the water content did not change and the filling

reached the state of full water). After saturation, each group of test pieces were weighed and recorded. Each group prepared 3 filling body test pieces. The average water content of 4 groups of filling body test pieces was shown in Table 1. The moisture content of different filling body specimens can be calculated with the following equation:

$$\omega_c = \frac{m_c - m_d}{m_d} \times 100\% \quad (1)$$

where: ω_c was the water content of the filling body, %; m_c was the mass of filling body after different saturation degrees, g; m_d was the mass of the filled body after drying, g.

Table 1. Average moisture content of the four groups of coal-based solid waste paste filling.

Classification	Group A	Group B	Group C	Group D
Before saturation	312.56 g	304.73 g	305.41 g	302.81 g
After saturation	-	332.03 g	367.00 g	377.70 g
Moisture content	0	8.96%	20.17%	24.73%
Uniaxial compressive strength	2.999 MPa	2.521 MPa	0.903 MPa	0.545 MPa

2.3. Experimental Instruments and Procedures

The test system consists of loading equipment and acoustic emission monitoring equipment. The loading equipment adopted a TZW-500 microcomputer controlled electro-hydraulic servo rock direct shear apparatus. Its normal load was 0~300 kN, the normal overload protection was 2% of the overload, the normal working stroke was 0~100 mm, and the loading mode was two-way electro-hydraulic servo coincidence loading, fully automatic closed-loop control. The test system was shown in Figure 2.

After the specimen reached the curing age, the loading test was started. The test conditions and steps were carried out in accordance with the Standard for Test Methods of Mechanical Properties of Ordinary Concrete (GB/T500801-2002). The stress loading mode was used to slowly load to 0.1 kN, and then the displacement loading mode was used to load until the specimen was damaged. The loading rate was 0.05 mm/min. Four acoustic emission sensors were arranged at an interval of 90° from top to bottom on the sample surface of the filling body, the sampling frequency is 2.5 MHz, and the threshold value of acoustic emission signal acquisition was 40 dB. During the loading process, load and deformation parameters were recorded and collected.

3. Experimental Results and Analysis

3.1. Influence of Water Content on the Strength of Paste Filling

Uniaxial compressive strength was an important parameter to measure the quality of filling. Figure 3 shows the stress-strain curves of four different water content fillings during uniaxial compression.

As can be seen from Figure 3, with the increase of water content, the compressive strength of filling specimen gradually decreases. The strength of filling specimens 1 h, 2 h and 3 h with saturated water decreased by 15.97%, 69.90% and 81.83%, respectively, compared with that of dry specimens. The stress-strain curves of filling with different water contents were divided into compaction stage (I), elastic deformation stage (II), plastic deformation stage (III) and post-peak failure stage (IV). With the increase of water content, filling specimens gradually changed from brittleness to ductility.

In the compaction stage (I), the filling body in the dry state and the filling body in different water-containing states show similar stress-strain phenomena, and the stress-strain curves were basically coincident, which indicates that the filling body has experienced the same structural change in this stage, because there were many large “closed” pore structures in it, which prevent the invasion of water. These “closed” pores were almost not affected by the water-containing state when they were closed under pressure, it shows that the filling sample was not affected by moisture during compaction.

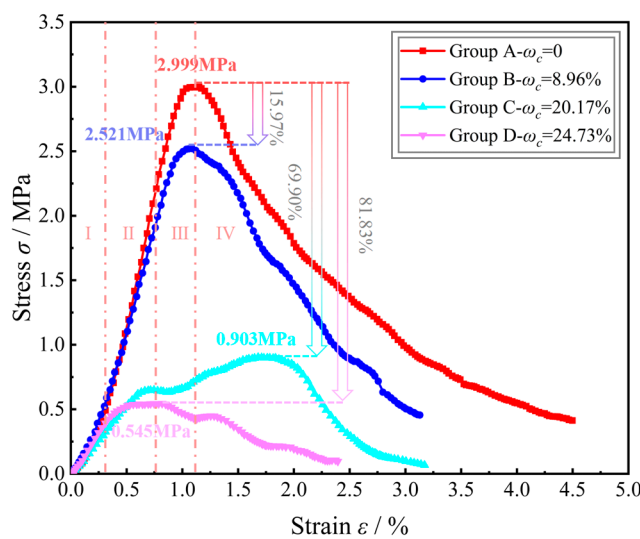


Figure 3. Stress-strain curves of filling body of coal-based solid waste paste with different moisture content.

In the elastic deformation stage (II), the curves of the filling body samples in the dry state and saturated for 1 h were basically consistent, indicating that the difference between their elastic moduli was small. However, with the increase of saturated time, the slope of the curve gradually decreases, and the elastic modulus decreases, indicating that the elastic modulus generally decreases with the increase of water content.

In the plastic deformation stage (III), the internal “closed” pores of the filling body specimen were further compressed and damaged, and the water gradually invades. It shows that the larger the water content was, the stronger the water invasion to the damaged pores was. It shows on the stress-strain curve that the filling body begins to change from brittleness to ductility with the increase of the water content.

In the post-peak failure stage (IV), after the filling body reaches the peak stress, its internal pores and fractures continue to expand, connect, and fuse, accompanied by the generation of new fractures, which ultimately leads to the failure of the filling body.

In the dry state, the stress-strain curve was smooth before and after the peak, no significant sudden drop was observed, and its elastic modulus was large. When the water content increased to 8.96%, there was no obvious fluctuation in the curve before the peak, and there were three irregular inflection points in the curve after the peak, indicating that the internal cracks of the filling body in this state continue to develop and connect after the peak, and large macro cracks were produced. When the water content was 20.17%, an inflection point appeared in the middle section of the curve before the peak, indicating that the original internal structure has been partially destroyed; new cracks appeared and recompacted, which showed that the stress-strain curve rises after the inflection point until the peak stress was reached. When the water content reached 24.73%, there were several irregular inflection points in the back-peak curve, indicating that the internal structure had multiple cracks developing and connecting, and producing macroscopic cracks. It can be inferred that the higher the water content, the greater the impact on the strength of filling specimen.

To more intuitively describe the change rule of filling body strength with water content, Figure 4 shows the change trend of filling body peak strength with water content. The quadratic function was used to fit the relationship between the peak strength of the filling body and the water content. The fitting correlation coefficient was 0.9498. The fitting result can better reflect the influence of the water content on the peak strength of the filling body. The fitting equation was:

$$\sigma_p = -20.78465\omega_c^2 - 5.43766\omega_c + 3.04507 \quad (2)$$

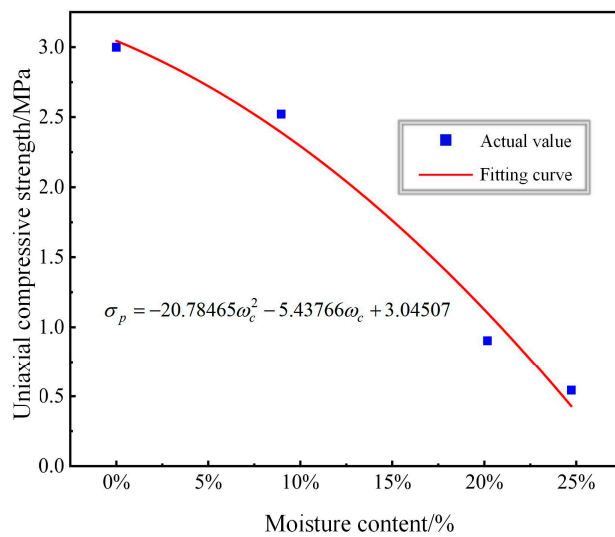


Figure 4. Relation curve between moisture content and uniaxial compressive strength of paste filling body.

3.2. Damage Constitutive Model of Paste Filling with Different Water Content

According to the strain equivalence principle proposed by Lemaitre (1971), it can be seen that the strain caused by the stress acting on the damaged filling was equivalent to the strain caused by the actual stress (effective stress) acting on the non-destructive filling [37]. If the filling body was regarded as an isotropic continuous medium, then:

$$\sigma = E\varepsilon(1 - D) \quad (3)$$

where: σ was the effective stress borne by the filling body; ε was the strain of the filling body; E was the elastic modulus of the filling body; D was the damage value of the filling body.

The stress-strain curve of the filling body obeys Weibull statistical distribution density function [38], which can establish a relationship between the damage and the defects contained in each micro element. Then, the damage value of the paste filling body under uniaxial compression was:

$$D = 1 - \exp\left[\frac{-(\varepsilon/\varepsilon_p)^\lambda}{\lambda}\right] \quad (4)$$

λ was the shape parameter of Weibull statistical distribution, which can be expressed as:

$$\lambda = 1 / \ln(E\varepsilon_p / \sigma_p)$$

where σ_p was the peak stress of the filling body, ε_p was the peak strain of the filling body.

By introducing Equation (4) into Equation (3), the damage constitutive equation of filling under uniaxial compression can be obtained:

$$\sigma = E\varepsilon \exp\left[\frac{-(\varepsilon/\varepsilon_p)^\lambda}{\lambda}\right] \quad (5)$$

According to Equation (2), the relationship between the peak stress of the filling body and the water content was a quadratic function, so the Equation (2) was introduced to obtain the Weibull statistical distribution shape parameters of the filling body under different water content: $\lambda_c = 1 / \ln[E\varepsilon_p / (A\omega_c^2 + B\omega_c + C)]$.

Taking λ_c into Equations (4) and (5), the damage evolution equation and damage constitutive equation of filling body with different water contents can be obtained. In combination with the stress-strain curves of four filling bodies with different water contents (Figure 3); the calculation results were shown in Table 2. According to the damage evolution equation and damage constitutive equation of coal-based solid waste paste filling with different

water content as shown in Table 2, the strain damage curve and stress strain curve of filling with different water contents can be drawn, as shown in Figures 5 and 6, respectively.

Table 2. Damage evolution equation and constitutive equation of filling with different moisture content.

Specimen	E/MPa	σ_{pc}/MPa	λ_c	Damage Evolution Equation	Damage Constitutive Equation
Group A	262.18	3.0451	4.4203	$D = 1 - \exp \left[\frac{-(\varepsilon/0.0115)^{4.4203}}{4.4203} \right]$	$\sigma = E\varepsilon \exp \left[\frac{-(\varepsilon/0.0115)^{4.4203}}{4.4203} \right]$
Group B	280.25	2.3910	1.5706	$D = 1 - \exp \left[\frac{-(\varepsilon/0.0109)^{1.5706}}{1.5706} \right]$	$\sigma = E\varepsilon \exp \left[\frac{-(\varepsilon/0.0109)^{1.5706}}{1.5706} \right]$
Group C	104.54	1.1027	2.1362	$D = 1 - \exp \left[\frac{-(\varepsilon/0.0168)^{2.1362}}{2.1362} \right]$	$\sigma = E\varepsilon \exp \left[\frac{-(\varepsilon/0.0168)^{2.1362}}{2.1362} \right]$
Group D	127.59	0.4292	1.1174	$D = 1 - \exp \left[\frac{-(\varepsilon/0.0082)^{1.1174}}{1.1174} \right]$	$\sigma = E\varepsilon \exp \left[\frac{-(\varepsilon/0.0082)^{1.1174}}{1.1174} \right]$

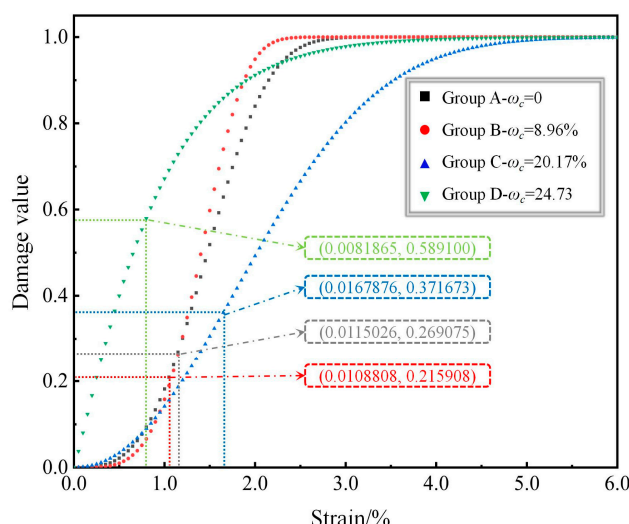


Figure 5. Variation curve of damage value of paste filling body.

The peak damage was defined as the damage value corresponding to the peak stress of the filling specimen. Figure 5 showed the coordinates of the peak strain and peak damage value corresponding to the peak strength of the filling body in each water-bearing state. It can be seen from Figure 5 that the filling body in all states reaches the peak strength when the strain is small. When the peak strength was reached, the peak damage value changes between 0.21 and 0.59. With the increase of water content, the peak damage value decreases first and then increases, indicating that the water content has a certain role in promoting the damage development of the filling body. At the initial stage of strain, the damage values of Group A, B and C fillings under the same deformation conditions show the phenomenon of Group C > Group A > Group B. By comparing the stress-strain curve, it can be seen that in the elastic stage, the curves of Group A and Group B were relatively close, but the elastic modulus of Group B was slightly higher than that of Group A. Therefore, at the initial stage of strain, it showed that the damage growth rate of Group A was greater than that of Group B. The stress-strain curve of Group C has an obvious inflection point before the peak, and the internal structure was partially damaged, resulting in its damage value at the initial strain stage being slightly greater than that of Group A and Group B. With the increase of strain, the damage value of filling in Group A, B and C began to show the phenomenon of Group B > Group A > Group C under the same deformation condition. This was because after the filling in Group B reached the peak stress, three irregular inflection points appeared in its post-peak curve, and the internal fissure further developed and coalesced and formed a large crack, leading to greater damage. However,

due to the increase of water content, the stress-strain curve of Group C shows obvious ductility, which slows down the development rate of damage. For Group D filling body, due to its small compaction stage and elastic stage, it reaches the peak stress under very little strain. There were two irregular inflection points on its post-peak curve, and the internal cracks further develop and connect, making its damage value slightly larger than that of Group A, Group B and Group C. It can be seen that with the increase of strain, the influence of water content on the damage of filling was gradually smaller.

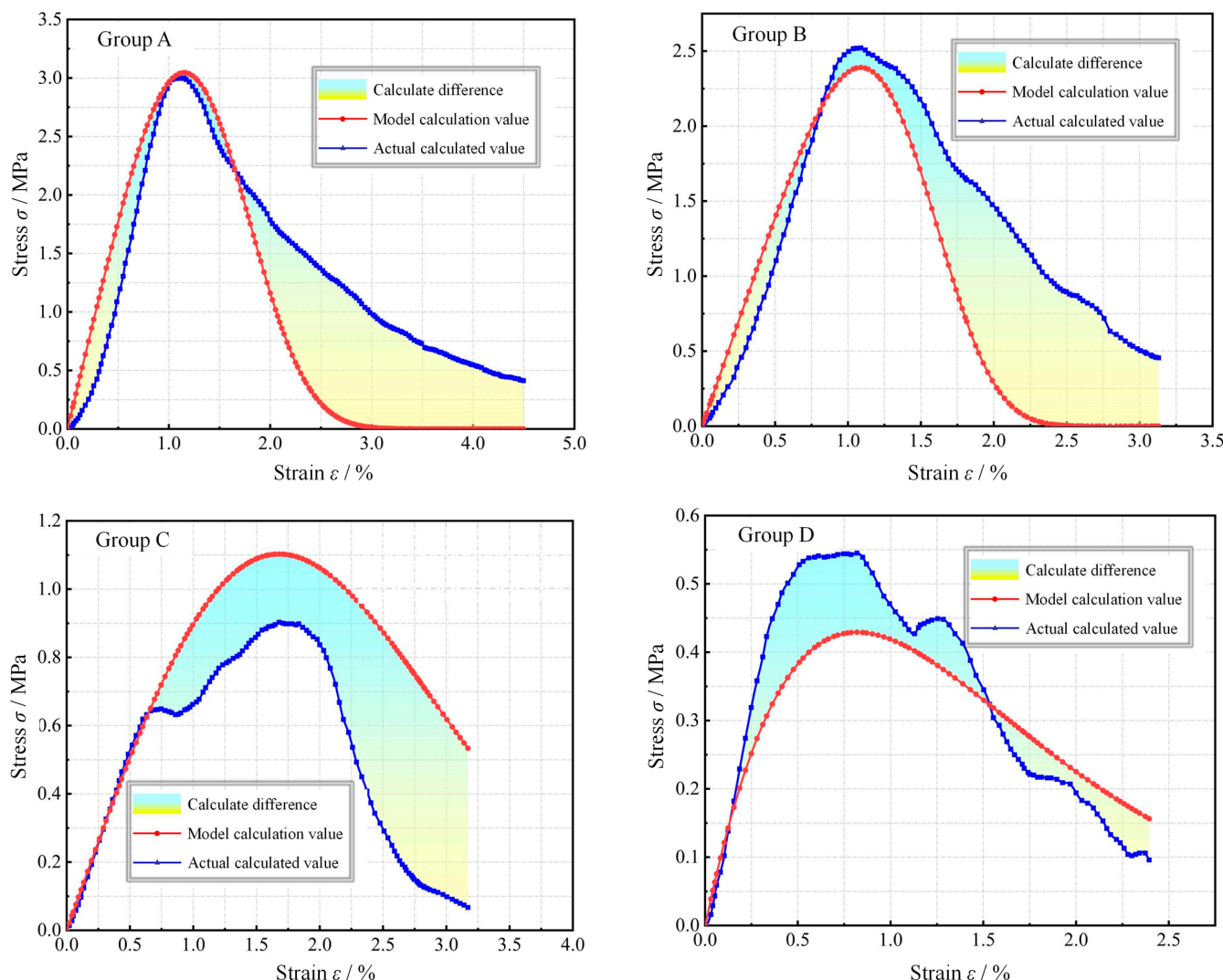


Figure 6. Comparison between experimental values and model values of stress-strain curves of paste filling body with different moisture content.

It can be seen from Figure 5 that the strain damage curve was “concave” before the damage reached peak damage, indicating that the growth rate of the damage value increases with the increase of strain; but after reaching peak damage, the strain damage curve starts to be “convex”, and the growth rate of the damage value slows down with the increase of strain at this stage.

According to Figure 6, before the peak stress, the actual value of the filling sample basically coincides with the model value. After the peak stress, with the increase of water content, the model curve was closer to the test curve. When the water content was 18% (saturation was 100%), the model curve and the test curve basically coincide. Compared with the completely dry filling sample, the calculated results have a higher agreement with the test results, and the higher the water content, the higher the agreement. It shows that

this damage-constitutive model was more suitable for the filling body with water. In the underground mining environment of a coal mine, due to the action of the humidity of the mining environment and groundwater, the filling body was always in a state of water, and the water content was generally large, close to the saturated state. Therefore, this damage-constitutive model has important practical engineering significance.

4. Discussion

To further analyze the mechanism of the influence of water content on the strength of filling, the author makes the following assumptions from the three aspects of physical effect, structural effect and chemical effect, based on the existing research results:

- (1) Physical effect: Water will reduce the friction between coal gangue, fly ash and cement cementation products in the filling body, resulting in the reduction of the force required for sliding between particles, which will lead to the failure of the filling body under low pressure (Figure 7).

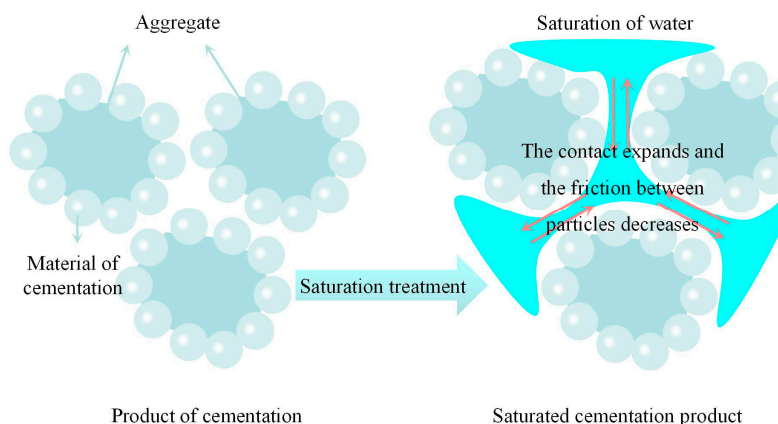


Figure 7. Physical effect of water saturation degree on strength of paste filling material.

- (2) Structural effect: There were microcracks in the filling body. When water entered the microcracks in the object, the microcracks accelerated to expand and develop into cracks when it was compressed, resulting in a decrease in structural strength (Figure 8).

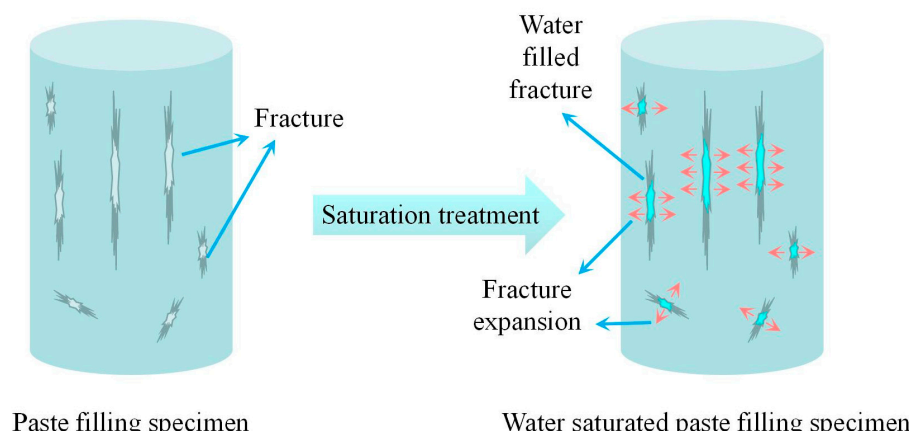


Figure 8. Structural effect of water saturation degree on strength of paste filling material.

- (3) Chemical effect: Chemical reaction between high content of water and materials in the filling body will lead to dissolution and destruction of some materials in the filling body, thus reducing the structural strength of the filling body (Figure 9).

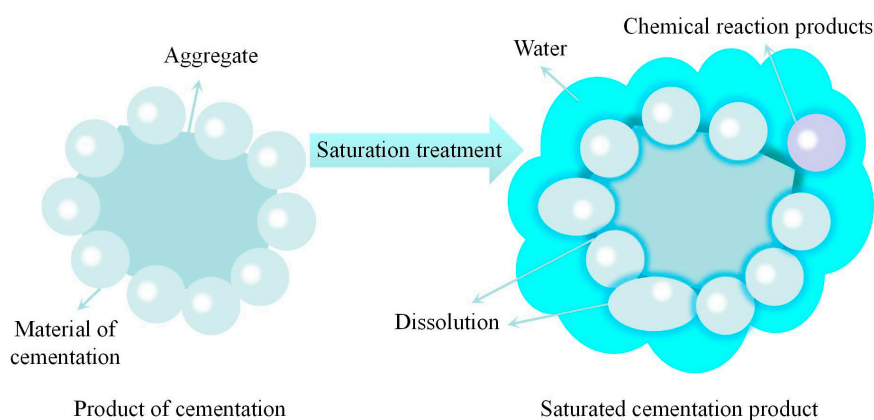


Figure 9. Chemical effect of water saturation degree on strength of paste filling material.

5. Conclusions

Through the analysis of strength characteristics and damage characteristics of coal-based solid waste paste filling materials with different water contents, the main conclusions were as follows:

- (1) With the increase of water content, the compressive strength of the filling specimen decreases gradually. And the higher the moisture content, the greater the impact on the strength of the filling sample.
- (2) The stress-strain curves of fillings with different water contents were divided into compaction stage (I), elastic deformation stage (II), plastic deformation stage (III) and post-peak failure stage (IV). With the increase of water content, the fillings gradually changed from brittle to ductile. The relationship between the water content and the peak strength was fitted by the binary linear equation, and the fitting results can better reflect the influence of the water content on the peak strength of the filling.
- (3) With the increase of strain, the influence of water content on the damage of the filling was gradually reduced. The evolution equation and constitutive equation of filling damage under different water content were established, and the reliability of the constitutive equation was verified by comparing the experiment with the model.
- (4) By discussing the water-bearing failure mechanism of paste backfill from the aspects of physics, chemistry and structure, it is clear that the water-bearing failure of backfill may be caused by the influence of water on the friction between particles, the expansion of micro-cracks and the generation of new hydration products. This study provides the direction for further research on the influence of water content on the strength and failure form of filling body.

Author Contributions: Methodology, X.H.; Formal analysis, M.W.; Writing—original draft, M.W.; Writing—review & editing, M.W. and K.Y.; Supervision, X.H.; Funding acquisition, X.H. All authors have read and agreed to the published version of the manuscript.

Funding: This research was funded by Scientific Research Foundation for High-level Talents of Anhui University of Science and Technology (2021yjrc11), Key Basic Research Project of China (2019YFC1904304), Institute of Energy, Hefei Comprehensive National Science Center (No.21KZS217), National Natural Science Foundation of China (52130402).

Institutional Review Board Statement: Not applicable.

Informed Consent Statement: Not applicable.

Data Availability Statement: Not applicable.

Acknowledgments: This paper was supported by the National Program on Scientific Research Foundation for High-level Talents of Anhui University of Science and Technology (2021yjrc11), Key Basic Research Project of China (2019YFC1904304), Institute of Energy, Hefei Comprehensive National Science Center under Grant No.21KZS217, National Natural Science Foundation of China (52130402).

Conflicts of Interest: The authors declare no conflict of interest.

References

1. Feng, G.R.; Du, X.J.; Guo, Y.X.; Qi, T.Y.; Wang, Z.H.; Li, Q.D.; Li, H.Y.; Kang, L.X. Basic theory of constructional backfill mining and the underground space utilization concept. *J. China Coal Soc.* **2019**, *44*, 74–84.
2. Chugh, Y.P.; Behum, P.T. Coal waste management practices in the USA: An overview. *Int. J. Coal. Sci. Technol.* **2014**, *1*, 163–176. [CrossRef]
3. Rybak, J.; Adigamov, A.; Kongar-Syuryun, C.; Khayrtdinov, M.; Tyulyaeva, Y. Renewable-Resource Technologies in Mining and Metallurgical Enterprises Providing Environmental Safety. *Minerals* **2021**, *11*, 1145. [CrossRef]
4. Zhang, C.; Li, B.; Song, Z.Y.; Liu, J.B.; Zhou, J.L. Breakage mechanism and pore evolution characteristics of gangue materials under compression. *Acta Geotech.* **2022**, *17*, 4823–4835.
5. Zhang, C.; Zhao, Y.X.; Bai, Q.S. 3D DEM method for compaction and breakage characteristics simulation of broken rock mass in goaf. *Acta Geotech.* **2022**, *17*, 2765–2781. [CrossRef]
6. Li, Y.L.; Lu, B.; Yang, R.S.; Lin, H.; Xu, B.; Wang, S.S.; Liu, C.H. Cemented backfilling mining technology with continuous mining and continuous backfilling method for underground coal mine and typical engineering cases. *J. China Coal Soc.* **2022**, *47*, 1055–1071.
7. Lin, H.; Yang, R.S.; Li, Y.L.; Lu, B.; Xu, B.; Fan, Z.Y.; Li, J.N. Application of short-wall continuous mining and continuous backfilling cemented-fill mining technology. *Chin. J. Eng.* **2022**, *44*, 981–992.
8. Xuan, D.Y.; Xu, J.L.; Wang, B.L. Green mining technology of overburden isolated grout injection. *J. China Coal Soc.* **2022**, *12*, 4265–4277. Available online: <http://kns.cnki.net/kcms/detail/11.2190.TD.20221128.1838.002.html> (accessed on 28 November 2022).
9. Wang, Z.Q.; Guo, X.F.; Gao, Y.; Chen, C.F.; Li, P.F.; Wang, L.; Zhao, J.L. Study of grouting technology of overburden-separation to reduce ground subsidence in Huafeng coal mine. *Chin. J. Rock Mech. Eng.* **2014**, *33*, 3249–3255.
10. Liu, J.G.; Li, X.W.; He, T. Application status and prospect of backfill mining in Chinese coal mines. *J. China Coal Soc.* **2020**, *45*, 141–150.
11. Yang, K.; Wei, Z.; Zhao, X.Y.; He, X.; Zhang, J.Q.; Ji, J.S. Theory and technology of green filling of solid waste in underground mine at coal power base of Yellow River Basin. *J. China Coal Soc.* **2021**, *46*, 925–935.
12. Wu, A.X.; Yang, Y.; Cheng, H.Y.; Chen, S.M.; Han, Y. Status and prospects of paste technology in China. *Chin. J. Eng.* **2018**, *40*, 517–525.
13. Yang, K.; Zhao, X.Y.; Wei, Z.; Zhang, J.Q. Development overview of paste backfill technology in China’s coal mines: A review. *Environ. Sci. Pollut. Res.* **2021**, *28*, 67957–97969. [CrossRef]
14. Zhao, Y.L.; Liu, Q.; Zhang, C.S.; Liao, J.; Lin, H.; Wang, Y.X. Coupled seepage-damage effect in fractured rock masses: Model development and a case study. *Int. J. Rock Mech. Min. Sci.* **2021**, *144*, 104822. [CrossRef]
15. Liu, Q.; Zhao, Y.L.; Tang, L.M.; Liao, J.; Wang, X.G.; Tan, T.; Chang, L.; Luo, S.L.; Wang, M. Mechanical characteristics of single cracked limestone in compression-shear fracture under hydro-mechanical coupling. *Theor. Appl. Fract. Mech.* **2022**, *119*, 103371. [CrossRef]
16. Kongar-Syuryun, C.; Aleksakhin, A.; Khayrtdinov, A.; Tyulyaeva, Y. Research of rheological characteristics of the mixture as a way to create a new backfill material with specified characteristics. *Mater. Today Proc.* **2021**, *38*, 2052–2054. [CrossRef]
17. Yin, S.H.; Hou, Y.Q.; Yang, S.X.; Zhang, M.Z.; Cao, Y. Analysis of deformation failure and energy dissipation of mixed aggregate cemented backfill during uniaxial compression. *J. Cent. South. Univ.* **2021**, *52*, 936–947.
18. Hou, Y.Q.; Yin, S.H.; Cao, Y.; Dai, C.Q. Research on Damage and Energy Dissipation Characteristics of Cemented Backfill under Different Loading Rates. *J. Hunan Univ.* **2020**, *47*, 108–117.
19. Hou, Y.Q.; Yin, S.H.; Cao, Y.; Dai, C.Q. Analysis of damage characteristics and energy dissipation of cemented tailings backfill with different curing ages under uniaxial compression. *J. Cent. South. Univ.* **2020**, *51*, 1955–1965.
20. Feng, G.R.; Xie, W.S.; Guo, Y.X.; Guo, J.; Ran, H.Y.; Zhao, Y.H. Effect of early load on mechanical properties and damage of cemented gangue backfill. *Chin. J. Rock Mech. Eng.* **2022**, *41*, 775–784.
21. Guo, Y.X.; Zhao, Y.H.; Feng, G.R.; Ran, H.Y.; Zhang, Y.J. Study on damage size effect of cemented gangue backfill body under uniaxial compression. *Chin. J. Rock Mech. Eng.* **2021**, *40*, 2434–2444.
22. Zhao, Y.H.; Ran, H.Y.; Feng, G.R.; Guo, Y.X.; Fan, Y.J. Damage evolution and failure characteristics of cemented gangue backfill body with different height-width ratios under uniaxial compression. *J. Min. Saf. Eng.* **2022**, *39*, 674–682.
23. Hua, X.Z.; Chang, G.F.; Liu, X.; Yang, K.; Chen, D.H.; Li, C.; Wang, E.Q. Strength evolution law and acoustic-emission characteristics of multi-source coal-based filling body of solid wastes. *Chin. J. Rock Mech. Eng.* **2022**, *41*, 1536–1551.
24. Zhao, K.; Huang, M.; Yan, Y.J.; Wan, W.L.; Ning, F.J.; Zhou, Y.; He, Z.W. Mechanical properties and synergistic deformation characteristics of tailings cemented filling assembled material body with different cement-tailings ratios. *Chin. J. Rock Mech. Eng.* **2021**, *40*, 2781–2789.

25. Jin, S.B.; Liu, K.W.; Huang, J.; Jin, S.H. Study on Damage Constitutive Model of Backfill Under Uniaxial Compression Loading. *Gold Sci. Technol.* **2021**, *29*, 555–563.
26. Yang, X.L.; Wang, W.J. Shear failure characteristics of cemented interface between filling material and surrounding rock at different curing temperatures. *China Civil Eng. J.* **2022**, *55*, 76–87.
27. Jin, A.B.; Wang, J.; Chen, S.J.; Li, H. Strength and damage characteristics of tailings filling body with different particle size distributions. *Rock Soil Mech.* **2022**, *43*, 3083–3093.
28. Chen, S.M.; Wang, W.; Wu, A.X.; Wang, Y.M. Influence rules of curing stress on strength of cemented paste backfill materials and its mechanism analysis. *Chin. J. Nonferrous Met.* **2021**, *31*, 3740–3749.
29. Nie, Y.L.; Wang, X.J.; Huang, G.L.; Li, S.C.; Feng, X.; Cao, S.R. Strength and Damage Model Analysis of Pure Tailings Cemented Filling Body with Different Water Content. *Bull. Chin. Ceram. Soc.* **2018**, *37*, 2008–2013.
30. Li, Z.F.; Zhang, C.; Zhang, J.; Jin, Q.; Wang, Y.S.; Yan, N. Mechanical properties and damage mechanism of backfill with different water saturation. *J. Min. Saf. Eng.* **2021**, *38*, 1063–1069 + 107.
31. Wang, Y.Y.; Yu, Z.Q.; Cui, L.Z. Experimental study on compressive behavior of cemented paste backfill material with different water contents. *Coal Sci. Technol.* **2022**, *50*, 219–224.
32. Liu, D.; Xu, J.C.; Pu, H. Experimental study on creep characteristics of gangue cemented fillers with different water content. *J. Min. Saf. Eng.* **2021**, *38*, 1055–1062.
33. Ermolovich, E.A.; Ivannikov, A.L.; Khayrtdinov, M.M.; Kongar-Suryun, C.B.; Tyulyaeva, Y.S. Creation of a Nanomodified Backfill Based on the Waste from Enrichment of Water-Soluble Ores. *Materials* **2022**, *15*, 3689. [[CrossRef](#)]
34. Kongar-Suryun, C.; Tyulyaeva, Y.; Khairutdinov, A.M.; Kowalik, T. Industrial waste in concrete mixtures for construction of underground structures and minerals extraction. *Conf. Ser. Mater. Sci. Eng.* **2020**, *869*, 032004. [[CrossRef](#)]
35. Liu, W.Z.; Chen, J.T.; Guo, Z.P.; Yang, H.Z.; Xie, W.W.; Zhang, Y.D. Mechanical properties and damage evolution of cemented coal gangue-fly ash backfill under uniaxial compression: Effects of different. *Constr. Build. Mater.* **2021**, *305*, 124820. [[CrossRef](#)]
36. Liu, W.Z.; Guo, Z.P.; Wang, C.; Niu, S.W. Physico-mechanical and microstructure properties of cemented coal Gangue-Fly ash backfill: Effects of curing temperature. *Constr. Build. Mater.* **2021**, *299*, 124011. [[CrossRef](#)]
37. Lemaitre, J. How to use damage mechanics. *Nucl. Eng. Des.* **1984**, *80*, 233–245. [[CrossRef](#)]
38. Zhao, K.; Zhu, S.T.; Zhou, K.P.; Yan, Y.J.; Zhao, K.; Li, Q.; Gu, S.J. Research on mechanical properties and damage law of tantalum-niobium ore cemented tailings backfill. *J. Min. Saf. Eng.* **2019**, *36*, 7.

Disclaimer/Publisher’s Note: The statements, opinions and data contained in all publications are solely those of the individual author(s) and contributor(s) and not of MDPI and/or the editor(s). MDPI and/or the editor(s) disclaim responsibility for any injury to people or property resulting from any ideas, methods, instructions or products referred to in the content.